Optically Addressable Hybrid: Photoconducting Polymer - Liquid Crystal Panels

S. Bartkiewicz[a], K. Komorowska[a], A. Miniewicz[a], J. Parka[b] and F. Kajzar[c]
[a]Institute of Physical and Theoretical Chemistry, Wroclaw University of Technology, 50-370 Wroclaw, Poland
[b]Institute of Technical Physics, Military University of Technology, Warsaw, Poland
[c]DRT-LIST (Recherche Technologique), DECS/SE2M/LCOF, CEA Saclay, 91191 Gif sur Yvette Cedex, France

ABSTRACT

The performances of photorefractive hybrid panels made from photoconducting polymer and nematic liquid crystal layers are reviewed and discussed. Their properties were studied under pulsed and cw illumination. The dynamic holography experiments with pulsed laser beams give information on the charge mobility in the thin photoconducting layers. The use of panels to visualize the phase objects introducing small distortions to plane wave front (such as e.g. turbulence of air) through the well-known Zernike filtering is also shown. The advantage of such nonlinear Zernike filter over conventional one is that no precise optical adjustment is necessary and the filtering is relatively easy to control by tuning the externally applied field to the modulator and/or varying the incoming light intensity.

1. INTRODUCTION

Since its discovery [1] in ferroelectric single crystals $LiNbO_3$ and $LiTaO_3$ the photorefractive effect knows an increasing interest motivated mainly by a large number of practical applications, such as: coherent image amplification, real time holography, holographic time gating, dynamic optical memories, optical correlation for image recognition, incoherent – to coherent image transformation, novelty filtering, parallel beam processing, optical phase conjugation, optical interconnects and optical power limiting.

This variety of applications of photorefractive effect made a good stimulus for an important research on material development, a better comprehension of the phenomenon and device applications. Large number of inorganic crystals were shown as exhibiting this effect: pure or 3d metals doped compounds of the same family as lithium niobate: like $BaTiO_3$, $KNbO_3$, $KTa_{1-x}Nb_xO_3$, ferroelectric ceramics like $(Pb_{1-x},La_x)(Zr_y,Tiz)O3$ ($PLZT_{x/y/z}$), tungsten bronze type ferroelectrics (for a review see ref. [2]) such as $Ba_2NaNb_5O_{15}$, $BaSrNb_2O_6$, sillenites: $Bi_{12}GeO_{20}$ (BGO), $Bi_{12}TiO_{20}$ (BTO), $Bi_{12}SiO_{20}$ (BSO), III-V semiconductors: AsGa, AsIn, GaP, InP, InSb, II-VI binary semiconductors: CuCl, CdS, CdSe, CdTe, HgS, HgSe, HgTe, ZnS, ZnSe, ZnTe, ternary compounds such as: HgCdTe and CdZnTe , as well as multiple quantum wells (MQW's) composed from alternate epitaxial layers of semiconductors with different optical gaps, e.g. AsGa/AlAsGa, leading to the exciton confinement (cf. Nolte and Melloch [3]). However the single crystals are usually difficult to growth, are costly, with low damage threshold and its also difficult to obtain large surface single crystals (or films) for optical beam processing and the exponential gain coefficients are limited as well as the response time is usually long.

A dozen years ago researchers from IBM Almaden [4] reported first observation of the photorefractive effect in organic polymers. It is well known that these materials are low cost, easily processable, particularly into films and versatile. This discovery has done a large stimulus for the research withpolymers. Exponential gain coefficient as large as 220 cm^{-1} was reported [5]. However this result was obtained under a prohibitively high electric field of 90 V/μm and was characterized by a large response time of about 1s.

In order to exhibit the photorefractive effect the material has to show the following properties:

(i) Substantial charge mobility
(ii) Photosensitivity (light induced charge generation ability)
(iii) Linear (Pockels) electro-optic effect

In the case of photorefractive polymers these material requirements are satisfied by mixing molecules exhibiting adequate properties: charge conducting polymer (holes and/or electrons), photosensitizer and a non-centrosymmetric NLO chromophore in order to get the linear electro-optic (Pockels) effect. However, as it was shown by Moerner et al [6] the main contribution to the refractive index change in these polymers is coming from the high optical anisotropy of used

Organic Photonic Materials and Devices V, James G. Grote, Toshikuni Kaino, Editors,
Proceedings of SPIE Vol. 4991 (2003) © 2003 SPIE · 0277-786X/03/$15.00

NLO molecules and their rotational mobility under the applied electric field. Therefore another components are usually added to this composite material, i.e. a plasticizer, in order to decrease the glass transition temperature and increase in this way the rotational mobility of NLO chromophores. This explains the large values of electric field required when using these polymers as one has to rotate each molecule individually and the energy of interaction is small because of limited value of dipole moment (usually of few debyes) as compared to the thermal motion energy. In order to increase this "aligning" energy one has to increase the strength of the applied electric field. Based on these findings we have proposed recently [7] the use of nematic liquid crystals, known as having high rotational mobility due to large induced dipole moment of each domain and to separate the charge generation from the rotational part. In this paper we recall shortly the performances of this novel hybrid photorefractive structure and describe two practical applications: for charge mobility measurements through dynamic holography and as a nonlinear Zernike filter.

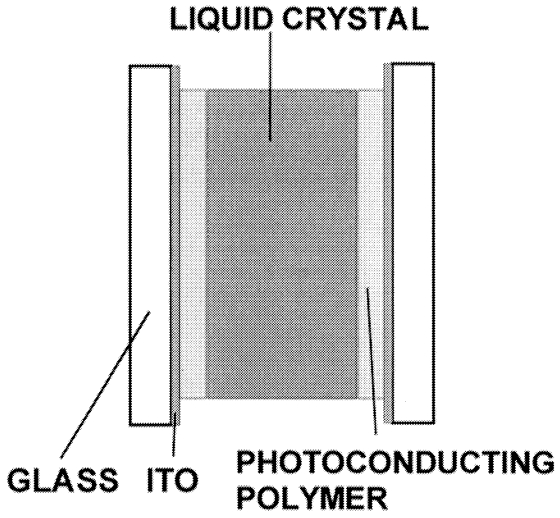

Figure 1: Schematic representation of the structure of photorefractive LC cell

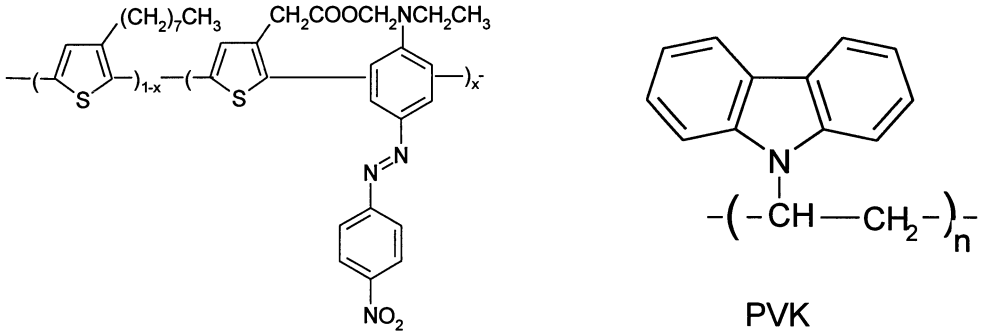

Figure 2: Chemical structure of the functionalized with Disperse Red 1 polythiophene copolymer and of PVK.

2. STRUCTURE AND PERFORMANCES OF PHOTOREFRACTIVE PANEL

The structure of the hybrid photoconducting polymer – liquid crystal panel (HPLCP) is shown schematically in Fig. 1. It consists of a nematic liquid crystal layer sandwiched between photoconducting polymeric layers. The photoconducting layers, deposited on semi-transparent ITO thin films, the last deposited on glass substrates ,are used also for anchoringof LC mesogens. Three types of photoconducting polymers were used: poly(3-octyl thiophene), poly(3-octyl thiophene) functionalized with Disperse red #1 and poly(N-vinyl carbazole) (PVK). All used polymers are known as good photoconductors [8]. In the case of PVK polymer the well known photosensitizer 2,4,7-trinitro-9-fluorenone (TNF) was

used, while poly(3-octyl)thiophene (POT) posses intrinsically this property. The operation wavelength is determined by the absorption spectrum of photosensitizer and spans between 400 – 630 nm for POT – DR#1 and 400-800 nm for PVK:TNF. The cells have typically thickness of ca. 10 μm. The polymer layers were uniaxially brushed in order to impose a planar ordering of nematic liquid crystal. The cells were filled with a multicomponent nematic liquid crystal mixture (E7) characterized by the static dielectric anisotropy $\Delta\varepsilon = +13.8$, extraordinary index of refraction n_o (589 nm) = 1.5211, n_e (589 nm) = 1.7464, birefringence, Δn (589 nm) = 0.2253 and viscosity $\gamma = 39$ (mm^2/s).

The performances of the panel were determined by the classical two-beam coupling experiments and are listed in Table 1 for the three photoconducting polymers used. Very large exponential gain coefficients were obtained, up to $\Gamma = 3700$ cm^{-1} for PVK:TNF (Fig. 3, the absolute amplification coefficient $g \approx 12$) with about three orders of magnitude weaker electric field required $E \approx 8$ kV/cm as compared to composite photorefractive polymers and a fast response time of 11 ms [9]. Obviously the amplification coefficient g (and Γ) depends on the applied voltage, grating period and the ratio of the intensities of two interfering beams (cf. Table 1).

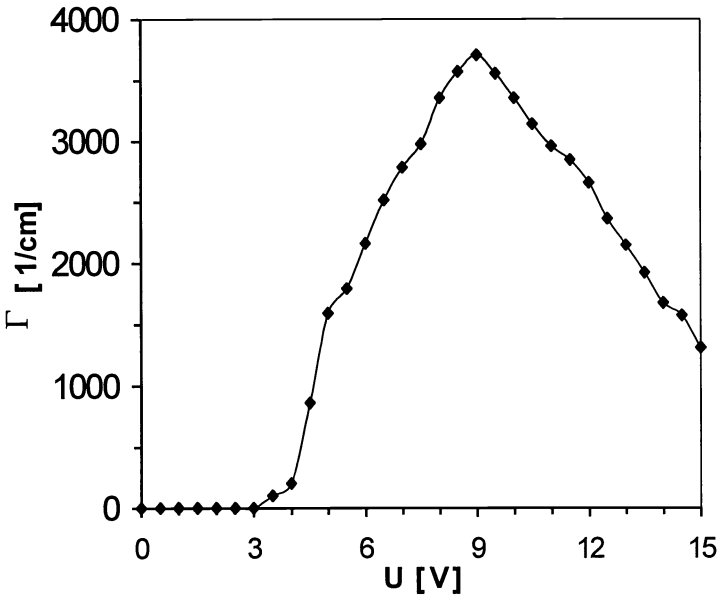

Figure 3: Variation of the exponential gain Γ with applied voltage for a 10 μm thick hybrid photoconducting polymer (PVK:TNF - 83:17) – LC panel.

Table 1. The maximum gain coefficients obtained using different photoconducting polymers

Photoconducting polymer	**Gain g**	**Exponential gain Γ (cm^{-1})**	**Electric field E (V/μm)**	**Incident beam power ratio m**	**Grating period Λ [μm]**
Poly(3-octyl thiophene)	3.5	930	0.6	10	15
Poly(3-octyl thiophene) – DR #1	7	2 600	0.6	10	30
PVK:TNF	12	3 700	0.9	12	15

Similarly as for the amplification coefficient the diffraction efficiency depends on the applied voltage as it is shown in Fig. 4 for the photoconducting composite PVK:TNF. It increases with the applied electric field, reaches a maximum and thereafter decreases. In this specific case that the diffraction efficiency

$$\eta = \frac{I_{1,diff}}{I_{o,inc}} \tag{1}$$

defined as the intensity of diffracted beam to incident beam intensity is very large in this specific case of PVK:TNF

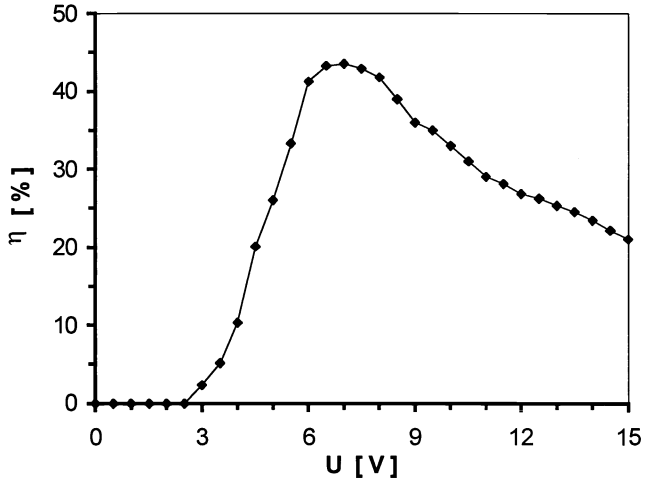

Figure 4: Diffraction efficiency η measured for a panel with photoconducting polymer (PVK/TNF : 83:17) as function of the applied voltage: the beam powers: $I_{O+} = I_{O-} = 10$ mW, angle between the beams $\theta = 1°$ and cell thickness d = 10 μm.

photoconducting polymer and E7 LC, is larger ($\eta_{max} \approx 45$ %) than that predicted by the Raman-Nath theory for thin holographic media ($\eta_{max} = 34$ %). For the other two photoconductors the observed maximum diffraction efficiency is lower: ($\eta \approx 26$ % for the panel with poly(3-octyl thiophene) and $\eta \approx 31$ % for poly(3-octyl thiophene) functionalized with DR1 (x = 0.12, cf. Fig. 2), as photoconductors, respectively (cf. Table 2). One of the possible explanations is the presence of strongly nonsinusoidal grating in PVK:TNF case which can be though of as a superposition of a number of sinusoidal gratings with periods Λ/2, Λ/3, Λ/4,....

Table 2. Best diffraction efficiencies measured for the studied photorefractive structures

Photoconducting polymer	Electric field (V/μm)	Diffraction efficiency %
Poly(3-octyl thiophene) POT	0.6	26
Poly(3-octyl thiophene) – DR #1	0.6	31
PVK:TNF(83:17)	0.8	45

3. DYNAMIC HOLOGRAPHY AND CHARGE MOBILITY

The HPLC panel was used for dynamic holography measurements [10], as shown in Fig. 5. Similar measurements were done on inorganic photorefractive single crystals by Biaggio and coworkers [11,12] to measure the charge carrier mobility in these materials, as the speed of grating formation and its erasure depends on it. The light source is a mode-locked Nd:YAG laser operating at 1064.2 nm, delivering pulses with 20ps time duration and 10 Hz repetition rate. After frequency doubling the 532 nm laser beam was split into two beams with equal intensities which were made interfering on the photorefractive panel by using two mirrors and well balanced optical paths (cf. Fig. 5). The generated refractive index grating in the panel was read by a cw He-Ne laser operating at 632.8 nm wavelength. The temporal evolution of the intensity of diffracted He-Ne beam was followed with a fast oscilloscope and is shown in Fig. 6. It follows that the main feature of the observed response signal points at least to three temporally distinguishable processes of refractive index grating formation, whose temporal occurrence depends on the applied voltage. It is obvious that the three processes must

depend on the charge carrier drift and diffusion in polymeric layer, ion transport within LC layer, characteristic reorientation times of LC molecules in electric field as well as thermal diffusion processes.

In the grating experiment involving photoconductivity and conductivity of the material the lateral (along the grating wavevector **q**) diffusion of charge carriers or ions must be taken into account. The simplest way to observe its influence is to perform an experiment in which the grating period is changed. From the measurements of diffraction signal evolution in function of grating spacing Λ we concluded that the positions in time of the diffraction maxima do not change at least within the Λ range of 2.5 μm to 11 μm. This suggests that the lateral charge carrier diffusion process is far less important for temporal evolution of electric space charge field build-up than charge carrier drift across the polymeric layer. However, we noticed the significant increase of the first order diffraction efficiency for higher periods Λ, which suggests that much larger index modulation amplitude Δn can be attained. The other process which predicts the strong temporal dependence on grating spacing Λ is connected with LC molecular reorientation mechanism with the time constant given by [13]

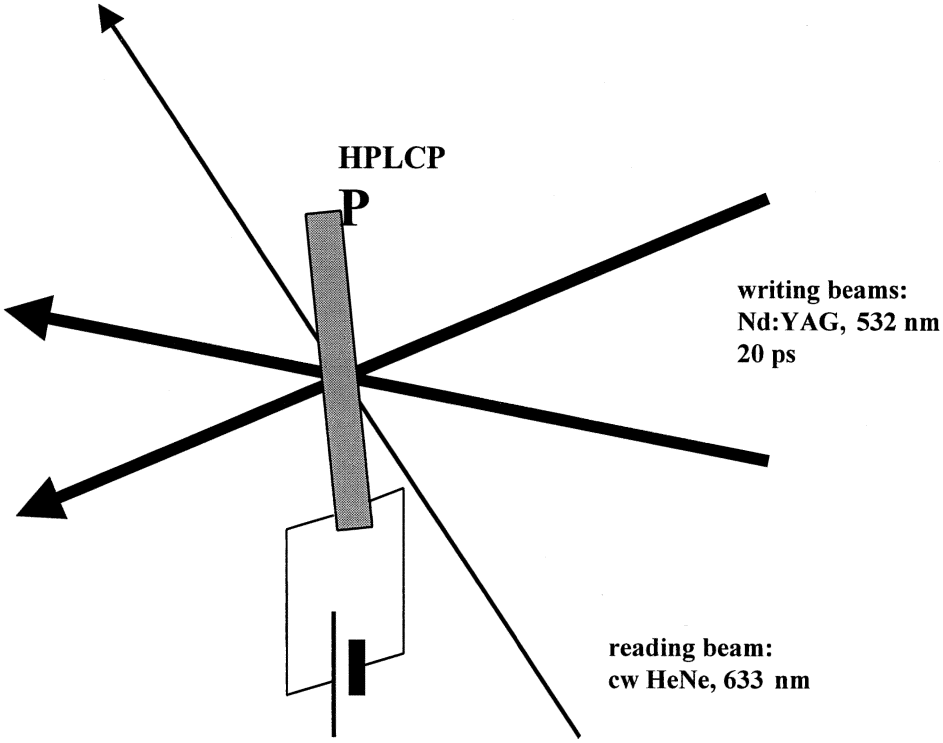

Figure 5: A schematic representation of experimental set-up for dynamic holography measurements in HCPLC panel. Two 20 ps beams write a grating read by a He-Ne (λ = 632.8 nm) laser

$$\tau_{el} = \frac{\gamma \cdot \Lambda^2}{4\pi^2 K} \qquad (2)$$

where γ is the rotational viscosity coefficient and K is the Frank elastic constant. On the basis of experiments we assume that the observed response time is not limited by molecular reorientation dynamics. We have ruled out the process connected with the possible heat production at the absorbing polymeric layer, this being in tens of μs time, thus too short to be observed in our experiments. Moreover, the observed temporal response of the system as function of pulse energy didn't evidence any change in positions on a time scale of the maxima of diffraction as function of incident beams energy, at least within the range of 30 - 340 μJ (in terms of exposure it corresponds to 0.95 - 10.8 mJ/cm^2) and only the diffraction efficiency increase was observed.

Thus the tentative explanation of the grating build-up was based on 3 consecutive charge grating formation processes (for details see Ref. [10]):

(i) The first peak, appearing about ~ 3 ms after 20 ps pulse is due to the charge grating created after the drift of holes (electrons are almost immobile due to the mobility about three orders of magnitude smaller) within both photoconducting polymeric layers. The positive charge is compensated at negatively biased ITO electrode and uncompensated charge (electrons) grating is created at the adjacent LC polymer layer. This process is thus determined by the hole mobility.

(ii) The uncompensated electrons initiate attract cations present in LC toward the negatively biased electrode causing a significant redistribution of electric field within the bulk of LC layer, which results in a build-up (~ 20 ms) of refractive index grating localized closer the positively biased electrode. A second maximum appears.

(iii) When the majority of the cations arrive to the negatively biased electrode (the LC-polymer interface) they compensate the interface charge in that region. It leads again to a novel redistribution of electric field in the LC layer (~ 60 ms) with refractive index grating located at the positively biased electrode, related to the spatial distribution of electrons within adjacent polymeric layer. Equilibrium happens when all the carriers produced initially by the Nd:YAG pulse are neutralized. The amplitude of the spatial modulation of space-charge electric field decreases to zero as well as light diffraction (~ 200 ms on average).

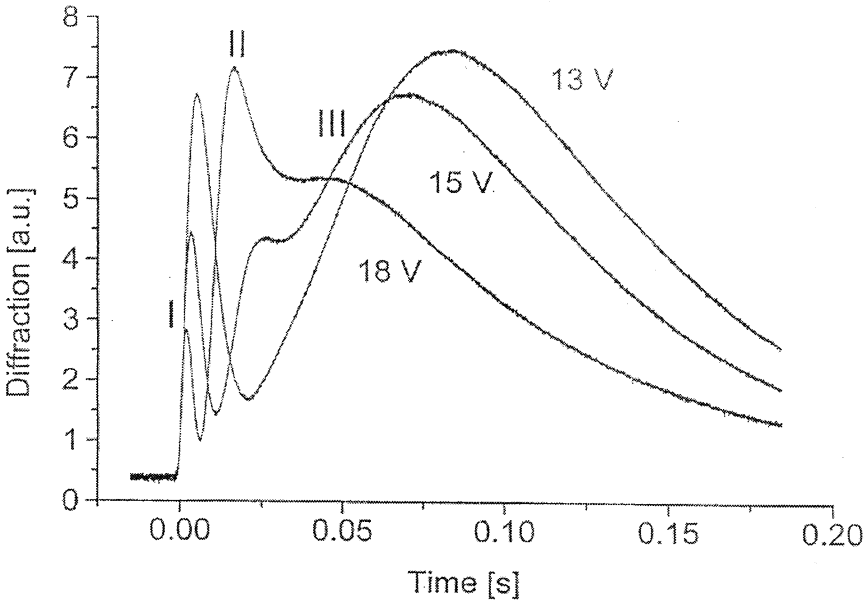

Figure 6: Typical temporal behavior of the first order diffracted HeNe beam intensity. Pulse energy of the Nd:YAG laser amounts to 0.34 mJ (10.8 mJ/cm^2) and voltage applied to the 10 μm thick panel was 13, 15 and 18 V, respectively.

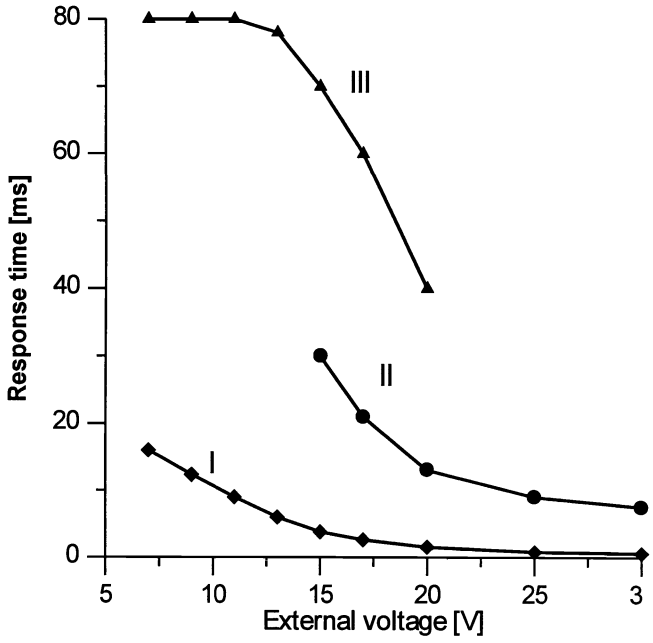

Figure 7: External field dependence of the temporal position of the three peaks (cf. Fig. 6) observed by HeNe laser. Labels I, II and III correspond to first, second and third peak, occurring in function of time.

Figure 7 shows the electric field dependence of different processes. Drawing such a dependence for the first phenomenon, related to hole mobility in polymeric layer in function of inverse of the applied electric field, as it is shown in Fig. 8 and assuming mean and uniform electric field across the LC layer and polymeric layers one can evaluate the hole mobility

$$\mu_h = \frac{\left(L_p / 2\right)d}{V \cdot t_I} \tag{3}$$

where L_p is the thickness of polymeric layer, V is the applied voltage, d is the thickness of the panel (LC layer) and t_I is the time at which the first peak occurs, one obtains the average value of the hole mobility equal to $\mu_h = 10^{-7}$ cm^2/Vs, which is comparable to that obtained by the other techniques [14,15].

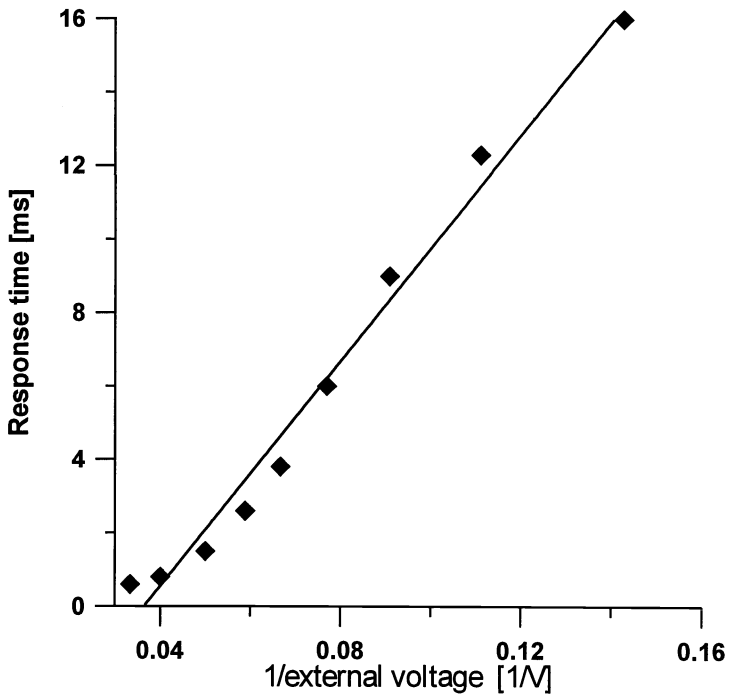

Figure 8: Temporal position of maximum I as function of the inverse of external field 1/V from which the average hole mobility in PVK:TNF polymer was calculated.

4. ZERNIKE FILTERING

A visualization of phase objects introducing small distortions to plane wave front (such as e.g. the turbulences of air) can be realized with the well-known Zernike filtering [16,17]. The used experimental set up is shown in Fig. 9. As it was shown by Zernike it is possible, by introducing a phase plate in the focal plane of a focusing lens, shifting the wave front phase by $\pm\frac{\pi}{2}$ (or any odd multiple of $\pm\frac{\pi}{2}$) to transform the phase objects (phase perturbations) into intensity objects (light amplitude distribution). However it requires the use of a precisely designed phase plate and works at one wavelength only. Recently Carhart et al. [18] have shown that by using an LC spatial light modulator (SLM) the Zernike type filtering can be also realized. By using developed by us HPLC panel we were also able to demonstrate very recently this kind of application [19]. The advantage of such nonlinear Zernike filter over conventional one is that no precise optical adjustment is necessary and the filtering is relatively easy to control by tuning the externally applied field to the modulator and/or varying the incoming light intensity.

The experimental set-up used for the phase visualization is shown in Fig. 9. It consists of an Ar^+ laser emitting polarized radiation at 514.5 nm wavelength. The input power of the laser was variable in the range of 1 μW to 10 mW. The initial laser beam was expanded and spatially filtered giving a collimated beam with gaussian intensity distribution with diameter of 2 cm. Then the beam passed through the phase object introducing a small dynamic phase distortions $\phi(x,y)$. The input lens produces a Fourier transformation i.e. the spatial spectrum of the object. The spectrum is filtered by an optical mask inserting a phase shift into zero order spectrum component centered around the optical axis due to nonlinear characteristic of the HPLC panel, placed into the Fourier plane perpendicularly to the optical axis (cf. Fig. 9). An asymmetric structure was used (cf. Fig. 1) with one side consisting of PVK:TNF 100 nm thick layer and the second one with a polyimide thin film. The LC layer was 10 μm thick. The PVK:TNF layer absorbs less than 4 % of the incident light intensity. The polymeric layers before assembling of the cell were rubbed in order to impose LC alignment, here a planar texture of nematic liquid crystal mixture.. Reverse Fourier conversion by the second lens reconstructs the image I (x', y') with the phase shift between these components. Alternatively an image in a far field was also observed and registered by a CCD camera (for details see Ref. [19]).

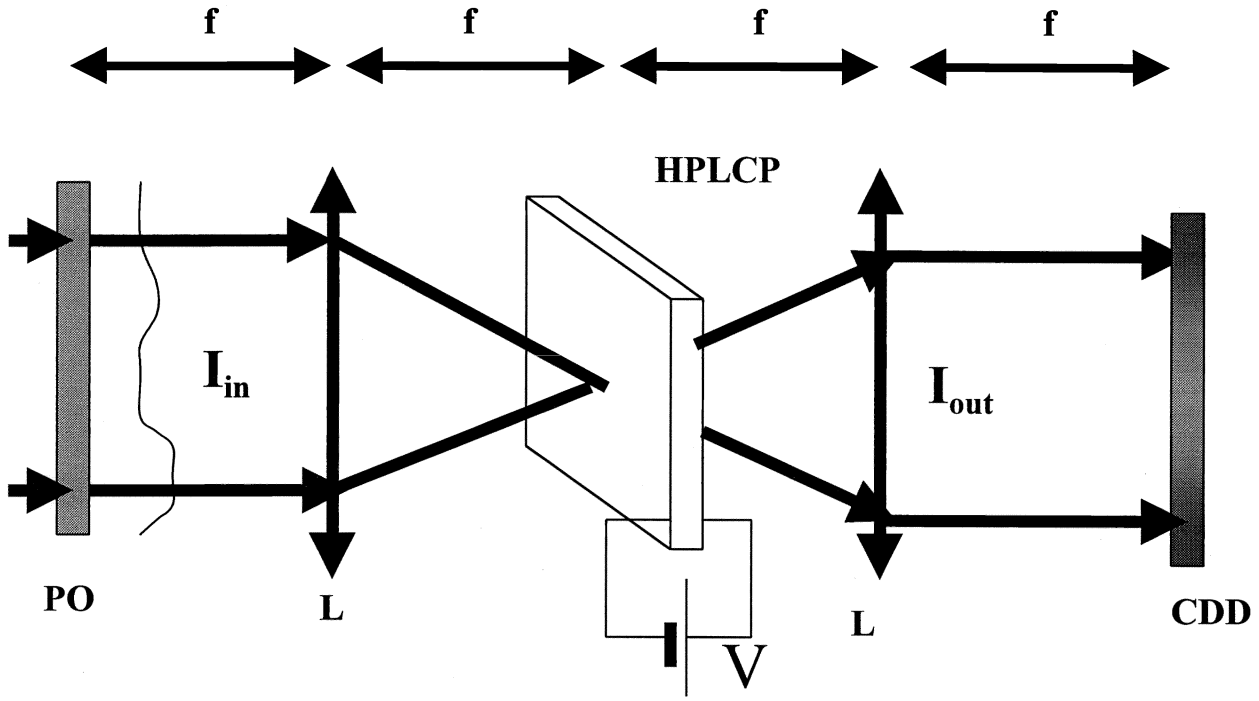

Figure 9: Schematic representation of the experimental setup for Zernike type filtering demonstration: PO – phase perturbing object, L – lense with focal length f, detector - CDD camera, V – voltage applied to HPLC panel.

The main advantage of such an NLO Zernike filter is that the response to light intensity I is usually highly nonlinear and can be tailored by changing the external voltage applied to the LC layer or using different liquid crystal mixtures, LC layer thicknesses and different sensitivity polymeric photoconducting layers. Generally, one can imagine two distinct optical systems using these structures as Zernike filters:
(i) phase image bearing beam itself induces a phase shift in the zero order spectrum component at a Fourier plane. This eliminates the need of alignment but requires the precise control of cell biasing voltage and/or incoming light intensity.
(ii) phase image bearing beam is transmitted through the NLO spatial light modulator without absorption and does not induce any refractive index change. The phase change equal to $\pi/2$ is induced by the external light illumination with properly focused beam inducing photoconductivity in the polymeric layer. The that setup is insensitive to the intensity of the image bearing beam but but it requires a precise optical alignment.

Figure 10 shows an example of nonlinear filtering enabling phase visualization due to air flow caused by heating of a the soldering-iron tip introduced at focal distance f in front of the first lens (cf Fig. 9). The technique enabled us to see the air fluctuations around the tip. The photographs were taken by Kodak CCD camera at total laser power of 2.4 μW at 514.5 nm. It is worth of noting that the dynamics of photoconductor-liquid crystal response has no influence on the monitoring of air-flow. It is sufficient that the light intensity at zero-order of the spectrum is able to induce the phase change equal $\pi/2$ and the nonlinear Zernike filtering is created. The light passing through the HPLC panel outside the zero-order does not involve any optical phase changes simply because its intensity is too small. In general this technique allows for a real-time tracing of air-flow peculiarities but it is not limited to the air-flows only but also to study the subtle phase changes in other media like transparent liquids or plastics caused by temperature or stress gradients

A visualization of a transparent thin glass plate showing phase variation of less than 0.4 π is demonstrated in Fig. 11. Adjustment of clear images was obtained by adjusting the voltage applied to the cell and the incident light intensity. Figure shows that not only a transparent plate (a corner) but even small variations in the plate thickness can be visualized.

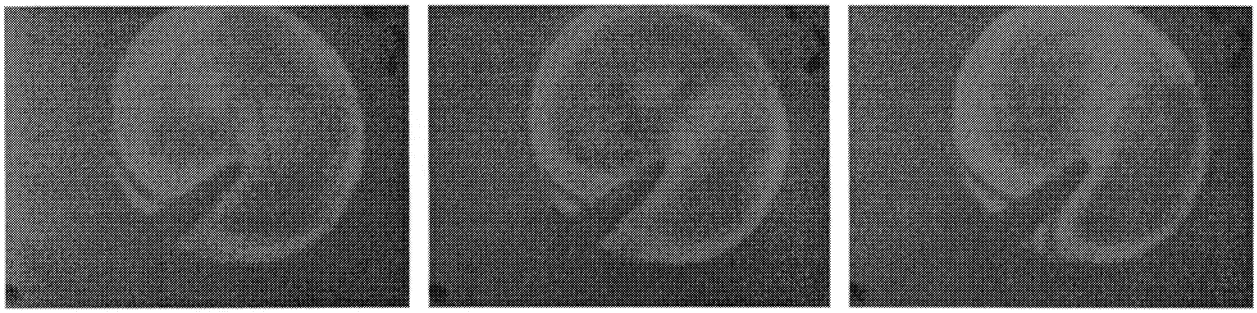

Figure 10: Experimental demonstration of air flow around a solder tip. The tip temperature is increasing gradually.

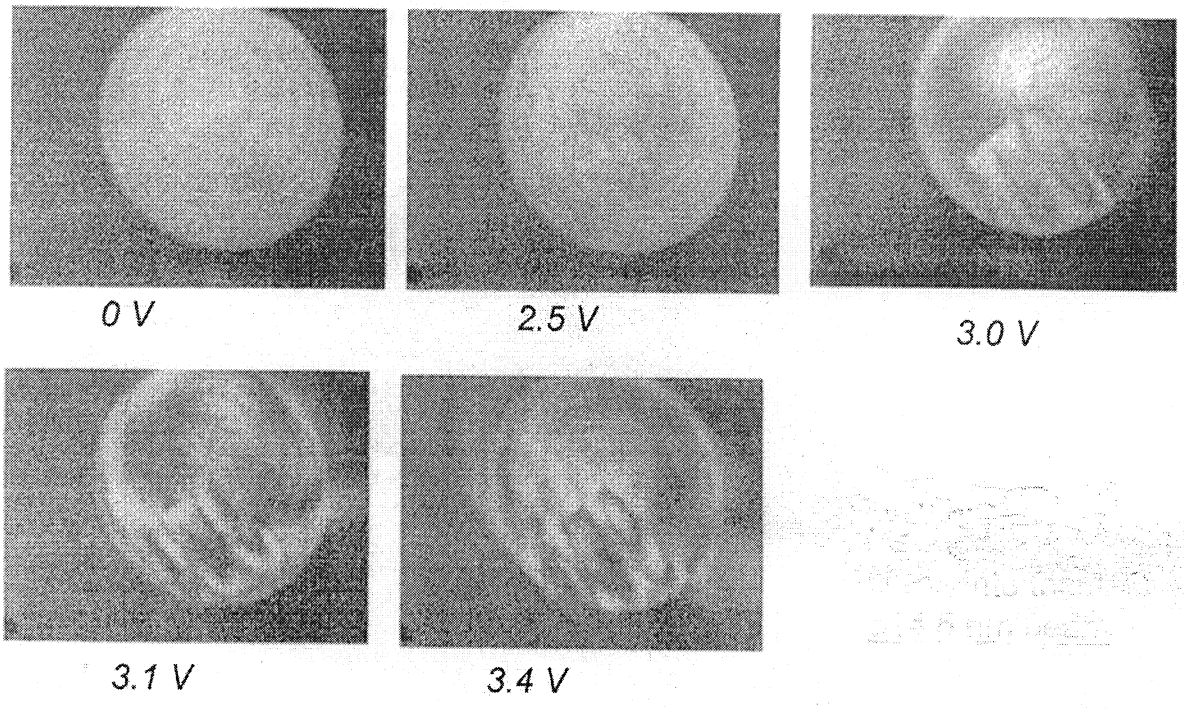

Figure 11: An example of visualization of a transparent plate (corner). The numbers correspond to the electric field strength applied to the cell.

6. CONCLUSIONS

The performances of the hybrid-photoconducting polymer – liquid crystal structures are shortly reviewed. They exhibit very interesting photorefractive properties such as a high absolute (g) amplification and exponential gain coefficients (Γ), the largest values obtained for a composite material PVK:TNF with $g = 12$ and $\Gamma = 3700$ cm^{-1}. The structures exhibit also large diffraction efficiencies; again the largest value ($\eta \approx 45$ %) being observed for a panel with photoconducting polymer (PVK/TNF, charged at 17 w% of TNF). This value is larger than the theoretical one predicted by Raman-Nath theory for thin media. These performances are obtained with a relatively low applied electric field, of 06-0.9 V/μm, about 3 orders of magnitude smaller than in the case of photorefractive composite polymeric materials. The response time is also significantly slower than in composite materials and is of about 10 ms.

Different practical applications of these panels were already demonstrated, such as optical correlator, beam amplification, optical limiting, incoherent – coherent beam transformation. In this paper we discussed two other applications such as dynamic holography and Zernike filtering. The dynamic holography gives information about the charge mobility in photorefractive media, as the grating formation depends on it. The Zernike filtering allows to visualize the phase objects. The used optically addressed HPLC panels are fully reversible optical elements, working at small light intensity levels (1 $\mu W/cm^2$ - 100 $\mu W/cm^2$) with relatively large spatial resolution 40 - 200 lines/mm and can be adjusted either by varying the applied voltage or the incident light intensity.

7. ACKNOWLEDGEMENTS

This research was partially supported by the Wroclaw University of Technology and partially by funds provided within Vth EC Framework project Adaptool.

REFERENCES

1. A. Ashkin, G. D. Boyd, J. M. Dziedzic, R. G. Smith, A. A. Ballman, J. J. Levinstein and K. Nassau, Optically Induced Trefractive Index Inhomogeneities in LiNbO3 and LiTaO3, *Appl. Phys. Lett.*, **9**, 72(1966)
2. R. R. Neurganokar and W. K. Cory, *J. Opt. Soc. Am. B,* **3,** 274(1986)
3. D. D. Nolte and M. R. Melloch, *Photorefractive Quantum Wells and Thin Films, in Photorefractive Effects and Materials*, D. D. Nolte Ed., Kluwer Academic Publ., Dordrecht 1995, Chapter 7.
4. S. Ducharme, J. C. Scott, R. J. Twieg and W. J. Moerner, Observation of the Photorefractive effect in a Polymer, *Phys. Rev. Lett.*, **66**, 1846(1991)
5. N. Peyghambarian, K. Meetholz, B. L. Volodin, Sandolphon and B. Kippelen, Organic Photorefractive Materials, *in Photoactive Organic Materrials: Science and Application*, F. Kajzar, V. M. Agranovich and C. Y.-C. Lee Eds, Kluwer Academic Publishers, Dordrecht 1995, pp. 281 - 292
6. W. E. Moerner, S. M. Silence, F. Hache and G. C. Bjorklund, *J. Opt. Soc. Am. B,* **11**, 320(1994).
7. S. Bartkiewicz, F. Kajzar, A. Miniewicz and M. Zagorska, Observation of High Gain in Liquid Crystal Panel with Photoconducting Polymeric Layers, *Appl. Optics,* 37, 6871(1998)
8. D. Althausen and P. Wunsche, *Mol. Cryst. Liq. Cryst.* **229**, 175 (1993).
9. A. Miniewicz, S. Bartkiewicz and F. Kajzar, On the Dynamics of Coherent Amplification of Light Observed in Liquid Crystal Panel with Photoconducting Polymeric Layers, *Nonl. Optics,* **19**, 157(1998)
10. S. Bartkiewicz, A. Miniewicz, B. Sahraoui and F. Kajzar, Dynamic Charge-Carrier-Mobility Mediated Holography in Thin Layers of Photoconducting Polymers , *Appl. Phys. Lett.*, **81**, 3705(2002)
11. I. Biaggio, M. Zgonik, P. Günter, *J. Opt. Soc. Am. B* , **9**, 1480(1992).
12. I. Biaggio, P. Günter, *Ferroelectrics,* **223**, 397 (1999).
13. I.-C. Khoo, *Liquid Crystals, Physical Properties and Nonlinear Optical Phenomena*, John Wiley & Sons Inc., New York, 1995.
14. W.D. Gill, *J. Appl. Phys.,* **43**, 5033(1972).
15. S. Serak, A. Kovalev, A. Agashkov, *Opt. Commun.* **181**, 391(2000).
16. F. Zernike, Diffraction theory of knife-edge test and its improved form, the phase contrast, *Mon. Not. R. Astron. Soc.* **94**, 371(1934)
17. F. Zernike, How I discovered phase contrast, *Science,* **121**, 345(1955)
18. G. W. Carhart, M.A. Vorontsov and E.W. Justh, Opto-electronic Zernike filter for high-resolution wavefront analysis using a phase-only liquid crystal spatial light modulator, *Proc. SPIE*, **4124,** 138-147(2000)
19. K. Komorowska, A. Miniewicz, J. Parka and F. Kajzar, Self – Induced Nonlinear Zernike Filter Realized with Optically Addressed Liquid Crystal Spatial Light Modulator, *J. Appl. Phys.*, **92**, 5635-41 (2002)